International Journal of Computer Vision 63(1), 45–64, 2005

Determining the Geometry of Boundaries of Objects from Medial Data*

JAMES DAMON
Department of Mathematics, University of North Carolina at Chapel Hill, Chapel Hill, NC 27599-3250, USA
jndamon@email.unc.edu

Received July 18, 2003; Revised July 16, 2004; Accepted July 16, 2004

First online version published in December, 2004

Abstract. We consider a region Ω in $\mathbb{R}^2$ or $\mathbb{R}^3$ with generic smooth boundary $\mathcal{B}$ and Blum medial axis M, on which is defined a multivalued "radial vector field" U from points x on M to the points of tangency of the sphere at x with $\mathcal{B}$. We introduce a "radial shape operator" S_{rad} and an "edge shape operator" S_E which measure how U bends along M. These are not traditional differential geometric shape operators, nonetheless we derive all local differential geometric invariants of $\mathcal{B}$ from these operators.

This allows us to define from (M, U) a "geometric medial map" on M which corresponds, via a "radial map" from M to $\mathcal{B}$, to the differential geometric properties of $\mathcal{B}$. The geometric medial map also includes a description of the relative geometry of $\mathcal{B}$. This is defined using the "relative critical set" of the radius function r on M. This set consists of a network of curves on M which describe where $\mathcal{B}$ is thickest and thinnest. It is computed using the covariant derivative of the tangential component of the unit radial vector field.

We further determine how these invariants are related to the differential geometric invariants of M and how these invariants change under deforming diffeomorphisms of M.

Keywords: Blum medial axis, skeletal structures, intrinsic geometry, relative geometry, radial shape operator, grassfire flow, radial flow, geometric medial map, relative critical set

Introduction

For 2D objects in $\mathbb{R}^2$ or 3D objects in $\mathbb{R}^3$ with (smooth) boundaries $\mathcal{B}$, the Blum medial axis M (Blum and Nagel, 1978), or an appropriate variant, is a fundamental object for describing shape. There has been a significant body of work devoted to methods for computing it, including the grassfire method (Kimia et al., 1990), the Hamilton-Jacobi skeleton (Siddiqi et al., 2002), and Voronoi methods (Szekely et al., 1994) among others.

Once we have the medial axis at our disposal, we may then work with it as if it were a basic object which can be manipulated, compared, deformed, or statistically analyzed as e.g. done by Pizer et al. (1999, 2003) and Yushkevich et al. (2002) etc. When such operations are applied to a medial axis, we would like to directly deduce geometric properties of the resulting boundary, including whether or not it remains smooth.

In this paper, we will determine how the geometric properties of $\mathcal{B}$ can be directly computed from medial data for the Blum medial axis M, including the question of smoothness. This will provide a *medial quantitative description* of geometric properties of objects, making precise typically descriptive terms for objects as being thick or thin, lopsided, or their having bulges or indentations.

Already M alone determines certain features such as protrusions, provided the corresponding curvature of the boundary changes sufficiently rapidly. However, for a variety of objects which have approximately the same Blum medial axis, there are significant differences in shapes arising from variations in the radius function. These may involve differences in the intrinsic

*Partially supported by National Science Foundation grants DMS-0103862 and DMS-0405947.

geometry, e.g. the sign of the Gaussian curvature, differential geometry such as principal curvatures and directions, and "relative geometry"such as identifying regions where Ω is thickest or thinnest.

In the generic case, the medial axis M itself is a "branched manifold" (which can be described more formally as a "Whitney stratified set"). Associated to it is a multivalued radial vector field U from points of M to the corresponding points of tangency on the boundary, and the radial distance function $r = ||U||$. There is the associated (multivalued) unit vector field U_1 such that $U = rU_1$. As well there are differential geometric properties of M, and natural orthonormal frames on M can be constructed from r (see Pizer et al., 2003). How do we extract *intrinsic medial structures* from this medial data which explicitly determine the geometric properties of $\mathcal{B}$?

One natural approach has been to seek the relation between the differential geometry of the boundary and that of the (smooth part of the) medial axis using information about the radius function r and its derivatives. Results obtained by this approach include: curvature of boundary curves in the 2D case, originating with Blum and Nagel (1978); the Gaussian and Mean curvatures of boundary surfaces in 3D by Nackman and Pizer (1985) and Nackman (1982); and in the opposite direction, deriving differential geometric properties of the medial axis from the differential geometry of the boundary by Siersma et al. (1998) and Siersma (1998) and Van Manen (2003a, b). In both of the surface cases, the relationship actually involves the differential geometry of a parallel surface of the boundary (rather than the boundary itself).

We shall determine the differential geometry of the boundary, in any dimension, directly from medial structures we introduce; however, we take what appears to be a counterintuitive approach to this problem by not explicitly involving the differential geometry of the medial axis itself Damon (2003) and Damon (2004).

The pair (M, U) consisting of the Blum medial axis and associated multivalued radial vector field is a special case of a "skeletal structure" which satisfies additional conditions, see Fig. 1. For a skeletal structure (M, U), we define "radial and edge shape operators" S_{rad} and S_E, and a "compatibility 1-form" η_U. These "shape operators" determine the "geometric properties of the radial vector field U_1" relative to M and are defined using only the first derivatives of U_1. The shape operators together with the radius function r allow us to determine the differential geometry of the boundary in the Blum case. We transfer information provided by these medial operators to geometric properties of the boundary via a "radial flow", which is a backwards version of the "grassfire flow" (Kimia, 1990) and yields a radial map from M to the associated boundary.

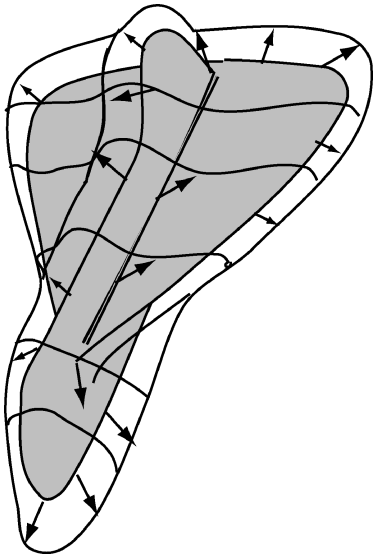

Figure 1. Blum medial axis and radial vector field for an object.

To begin, we apply the dimension independent results from Damon (2003) and Damon (2004) to 2D and 3D objects to give explicit formulas for the differential geometric shape operator for the object boundary (Theorem 3.1). For points corresponding to non-edge points of M, the formula is in terms of the radial shape operator, while at "crest points", which correspond to edge points of M, the formula is in terms of the edge shape operator (Theorem 3.4). We deduce explicit formulas for both the principal curvatures and principal directions for the boundary. Thus, we deduce all intrinsic and extrinsic differential geometry of the boundary using the radial and edge shape operators.

Second, we introduce a "geometric medial map" on the medial axis which identifies both intrinsic and "relative geometry" of the corresponding regions on the object boundary. This map can be thought of as the analogue of a weather map which provides information about the atmosphere above a region of the earth. A weather map typically shows regions of high and low pressure, curves of constant temperature, and arrows indicating wind direction, all exhibited on a map of that region on the ground. In an analogous fashion, the

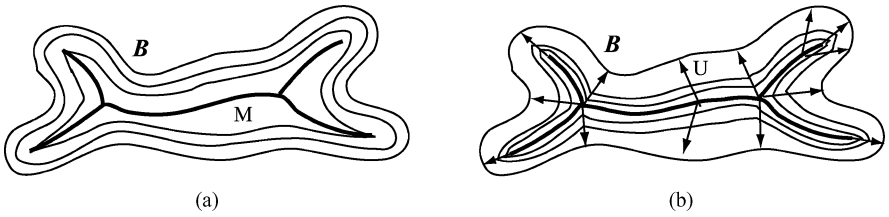

Figure 2. Radial flow versus grassfire flow between the boundary B and the medial axis M (darkened branch curve), (a) Shows levels of the grassfire flow, (b) Shows levels of the radial flow evolving along the multivalued radial vector field U.

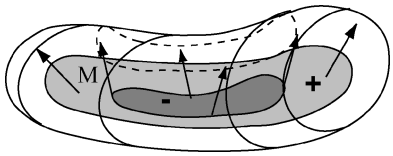

Figure 3. Part of the intrinsic geometric medial map on the blum medial axis M, showing regions of positive and negative radial curvature on one side of M, which correspond to regions of positive and negative gaussian curvature of one side of the region boundary.

geometric map on the medial axis will provide geometric information about the boundary, but its measurements only involve the unit radial vector field on the medial axis.

We need only use the radial shape operator S_{rad} to construct the "intrinsic geometry portion" of the geometric medial map. Since S_{rad} depends upon the choice of a value of U_1, for each side of each smooth sheet of M there will be a different S_{rad}. Thus, the intrinsic portion of the geometric medial map will be different on each side of a smooth sheet of M. Although S_{rad} is not a differential geometric shape operator and is not even symmetric, we treat it as if it were and introduce analogous terminology: det (S_{rad}) is the "radial curvature"; the eigenvalues and eigendirections of S_{rad} are "principal radial curvatures and directions"; the curves with tangent lines the principal radial directions are "principal radial curves" on M, etc. The geometric medial map on each side of a smooth sheet of the medial axis M consists of the following objects: regions of positive and negative radial curvature separated by radial parabolic curves, distinguished radial umbilic points, and at each point pairs of principal radial directions with principal radial curves, with the signs of the principal radial curvatures. What is surprising is that under the radial map these properties correspond to the same differential geometric properties on the object boundary (Theorem 4.2). More specific numerical geometric information can be added with the inclusion of r (Theorems 3.1 and 3.4).

The second portion of the geometric medial map captures relative geometry of the boundary. Already relative geometry on the medial axis appears when we seek to compare the sizes of principal curvatures of the boundary at distinct points or determine how principal curvatures change along curves. This cannot be done solely in terms of principal radial curvatures alone, but also involve r as expressed by the *radii of curvatures equation* (see Section 5). The properties of r as a function on M are key to relative geometry of the boundary.

For example, if we are asked where an object such as an egg or a potato is thickest, we would not choose along the long axis where it has the greatest diameter, but rather where the width is greatest relative to the central axis of the object. This is relative as opposed to intrinsic geometry. We introduce on the smooth sheets of M a discrete network of curves along which r is relatively largest and smallest (ridges of thickness and valleys of thinness) and where these properties undergo transitions. This system is defined using the "relative critical set" of r. This extends the notion of "ridge of a function", defined by Pizer and Eberly (1998), Eberly (1996), to a complete set of relative critical data whose generic properties have been determined for functions on $\mathbb{R}^n$ for all n, see Damon (1998, 1999), Miller (1998) and Keller (1999).

In our case, we define the relative critical set of r on M_{reg}, the smooth part of M. This classification places one of four labels on each part of a curve indicating the behavior of the radial function r on that part. These properties are defined and capture relative geometric properties even in the non-Blum case. Since r is defined on the smooth sheets of M rather than Euclidean space, the definition involves the Hessian operator of r; however, the generic properties continue to hold by Damon (in preparation).

In the Blum case, we reduce the calculation of these curves to calculations involving the first derivative of $U_{1\tan}$, the tangential component of U_1. Specifically this involves the eigenvalues and eigenvectors of the

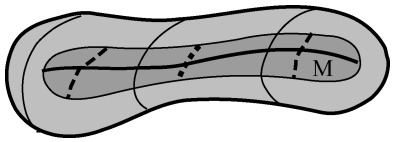

Figure 4. Relative part of a geometric map on the blum medial axis M showing the ridge curve of thickness (solid curve) and valley curve of thinness (middle dotted curve, along with connector curves (end dashed curves).

Hessian operator $H_r(v) = -\nabla_v U_{1\tan}$. In the Blum case, both r and $U_{1\tan}$ are single–valued at smooth points of M. Thus, the relative critical set has the same structure on each side, and hence is intrinsic to each smooth sheet of M. For example we see in Fig. 4, the ridges and valleys along with the connector curves indicating where the object is thickest and thinnest and where transition behavior occurs. The added data of the critical behavior of r on the relative critical set completely determines the thickness properties of the object.

When these two parts of the geometric map are combined, they give a precise decomposition of the medial axis which reflects via the radial map both the intrinsic and relative geometric properties of the object boundary.

We conclude by considering the effect on the associated boundary of distorting or deforming the Blum medial axis by a diffeomorphism. This effect is determined through the introduction of distortion operators which determine how the radial and edge shape operators are changed as a result of the diffeomorphism. This allows us to determine the smoothness and geometry of the new boundary in terms of the original shape operators and the distortion operators.

Finally we mention that in Damon (for publication) we show how the radial shape operator plays a fundamental role in computing global invariants of Ω and $\mathcal{B}$ as "skeletal and medial integrals" on M.

This author would like to especially thank Stephen Pizer and his students Paul Yushkevich and Tom Fletcher, whose original work concerning the geometric and smoothness properties of the boundary in terms of the differential geometry of the medial axis in the Blum case, raised questions which led to the approach we present here.

1. Blum Medial Axis and the Radial Flow

We begin by briefly recalling the standard properties of the Blum medial axis of a region Ω with smooth boundary $\mathcal{B}$. First, we consider the properties that occur generically, i.e. for almost all Ω which do not otherwise satisfy any special symmetry conditions. These properties have been worked out in general by several workers besides Blum and Nagel (1978), including Yomdin (1981) (as a "central set"), Mather (1983) (as the Maxwell set for the "family of distance functions on the boundary"), Bruce et al. (1983) and Bruce and Giblin (1986), (for the more general symmetry set), and Bogaevski (2002) (for transitions under variations). A recent paper by Giblin (2000) very clearly describes the main properties, and Pizer et al. (2003b) surveys the properties in the multiscale context.

For generic 2D objects, the Blum medial axis consists of smooth curves which may branch or end Blum and Nagel (2002). For generic 3D objects the local structure is also specifically given. Here generic means "almost all" in a very precise mathematical sense (see e.g. Mather, 1983), so that a nongeneric region can be made generic by applying an arbitrarily small perturbation of the boundary, while a generic region remains generic under sufficiently small perturbations of the boundary. For such generic 3D regions, the Blum medial axis M consists of pieces of smooth surfaces which may either: join in a Y-shaped configuration along a branch curve; have edges; or have an edge appear (end) at a "fin creation point" (which is an example of an edge-closure point in Damon (2003)), or have a "6-junction" configuration where six smooth sheets come together along 4 Y-branch curves, as shown in Fig. 5. The part of M formed from smooth points is denoted

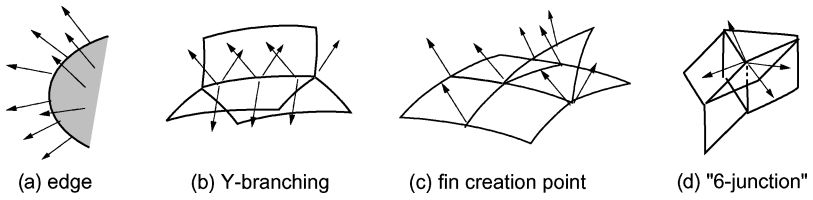

Figure 5. Possible local generic structures for blum medial axes in $\mathbb{R}^3$ and the associated radial vector fields.

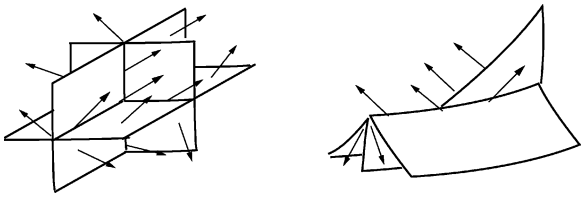

Figure 6. Possible nongeneric blum medial axes in $\mathbb{R}^3$.

M_{reg} while the set of points of M where the three nonsmooth possibilities occur is the singular set of M, denoted M_{Sing}. Although we shall describe results for the smooth case, the results continue to hold for M and U which are C^k for $k \geq 1$.

M as well satisfies additional properties describing how exactly the smooth sheets behave at singular points. These are described by M being a "Whitney stratified set" (see e.g., Mather, 1973 or Gibson et al., 1976) and more specifically a "skeletal set" (see Damon, 2003, Section 1). These extra conditions rule out possible exotic behavior that does not correspond to our intuitive ideas as presented in Fig. 5. However, in what we do here we allow nongeneric behavior as might result from finite symmetry as exhibited in Fig. 6.

On M is defined a multivalued *radial vector field* U from points of M to the corresponding points of tangency on the boundary, and *radial distance function* (or radius function) $r = ||U||$. For a smooth boundary $\mathcal{B}$, $r > 0$ so we may express $U = rU_1$, for a (multivalued) unit vector field on M. On smooth points of M (denoted M_{reg}), U has two values (called "sails" by Pizer et al. (2003a) in work on "M-reps"). At a singular point x_0 of M, the number of values of U is determined by the number of connected components (the "complementary components") into which M divides its complement in a small ball about x_0. For example, Y-shaped branch points have three local complementary components while fin creation points have two. For edge points of M (denoted ∂M), there is only a single value for U which is tangent to M and points away from M.

For a function or vector field to be differentiable on M requires the usual notion of differentiablity on M_{reg}. At points of M_{sing} which are not edge (closure) points, a smooth sheet of M can be extended smoothly through the branch curve. Then, for a function or vector field on the sheet to be differentiable at a point on the branch curve, it must also extend smoothly. At edge (closure) points, the usual notion of smoothness at an edge point of a surface no longer suffices. Tom Fletcher pointed

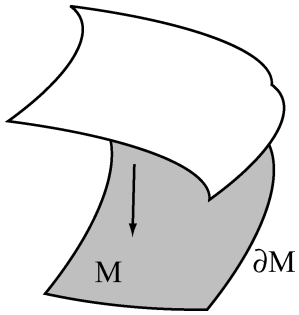

Figure 7. Projection defining an edge parametrization for edge of blum medial axis.

out that U will not be smooth in this sense. Instead, we must introduce *edge coordinates* as in Damon (2003), Section 1. These coordinates correspond to the projection of a half-parabolic surface as shown in Fig. 7. Then, as shown in Damon (2003), Example 1.5, for edge coordinates, both U and r are smooth at edge points. Of course Blum medial axes do not naturally come with these coordinates. Thus, we will state results at edges which use edge coordinates and then explain (in Section 2) how to use standard coordinates for surfaces with edges to compute objects such as the edge shape operator.

The pair consisting of the Blum medial axis together with the radial vector field, (M, U), forms a *skeletal structure* as defined in Damon (2003). For such a skeletal structure we define the *associated boundary* as $\mathcal{B} = \{x + U(x) : x \in M\}$ where we allow for each x all possible values of $U(x)$.

1.1. Radial Flow from the Blum Medial Axis

There is a way to relate the medial axis M and the boundary $\mathcal{B}$ by the *radial flow,* which is a backward version of the "grassfire flow" (Kimia, 1990) (also see Siddiqi and Bouix, 2002). Locally it is defined using a smooth value of U in some neighborhood of a point $x_0 \in M$ and given by the *local radial flow* $\psi_t(x) = x + tU(x)$. The time one value of this map defines a *radial map* ψ_1 (depending on the local choice of U) from a region of M to a corresponding region of $\mathcal{B}$. We note that as U is multivalued, the radial flow cannot be globally defined from M to $\mathcal{B}$ (instead it is globally defined on the "double of M", see Damon, 2003, Section 3).

We compare the radial flow versus the grassfire flow from the boundary to the medial axis. First, for the grassfire flow: (i) the flow is along normals to the boundary at unit speed; (ii) the level surfaces remain

normal to the lines of flow; (iii) the level sets are smooth manifolds while they are defined until shocks occur; (iv) then shocks occur at points of the Blum medial axis; (v) thus, for each point the flow is defined for a time that varies. By contrast, for the radial flow: (i) the flow is along the radial lines from the medial axis which correspond to normal lines to the boundary; (ii) the flow occurs at speeds which depend upon the radius function; (iii) the level sets $\mathcal{B}_t$ are not smooth but are stratified sets and only become smooth at the boundary; (iv) the level sets are not normal to the radial lines ; and (v) the flow is defined from all points of the medial axis for $0 \leq t \leq 1$ and reaches the boundary when $t = 1$.

Thus, we can think of the radial flow as "inflating the Blum medial axis" to fill out the region Ω, much as we inflate a balloon; with a crucial difference that the level surfaces $\mathcal{B}_t$ at time $t < 1$ fail to be smooth at all points coming from M_{sing}. Only at $t = 1$ do all of the singularities disappear and the level surface of the flow becomes the smooth boundary $\mathcal{B}$.

1.2. Compatibility 1-form and Compatibility Condition

Two key properties of the boundary are captured by a *compatibility condition* on the Blum medial axis. The *compatibility 1-form* η_U is defined by $\eta_U(v) = U_1 \cdot v + dr(v)$; this is multivalued because U is. M satisfies the *compatibility condition* at a point x_0 with smooth value U if $\eta_U = 0$ at x_0. Then, by Damon (2003), Lemma 6.1 or Damon (2004), Lemma 3.1,

Proposition 1.1. *The compatibility condition at a smooth point x_0 for the value U implies the orthogonality of U to the boundary at the associated boundary point*; *and the compatibility condition at a singular point x_0 for a value of U, implies that the boundary is weakly C^1 at the point associated to x_0 via U.*

Example 1.2 (Compatibility Condition for 2D Medial Axis). Let M be a 2D Blum medial axis. At a point x_0 on a branch curve γ of M, the compatibility condition has two implications. Both are consequences of (1.1) which follows from the compatibility condition.

$$dr(v) = -U_1 \cdot v = -U_{1\tan} \cdot v \qquad (1.1)$$

where $U_{1\tan}$ is the tangential component of U_1 for the smooth sheet in question and v is tangent to the sheet at x_0.

First, $U_1 \cdot v$ is independent of the choice of smooth value U at x_0 when v is tangent to γ (by (1.1) because r is uniquely defined on γ). Second, Eq. (1.1) also applies on each smooth sheet meeting γ, with v tangent to a smooth sheet at x_0 but normal to γ. The first condition fixes a common tangential projection onto γ for all values of U at the given point x_0.

The second gives independent conditions for the tangential component of each value of U_1 on each sheet. Let ∇r denote the "Riemannian gradient" of r as a function on M (see Section 6). Then the compatibility condition also asserts that on any smooth sheet the tangential component $U_{1\tan} = -\nabla r$. Hence, for v a unit vector and θ the angle between $U_{1\tan}$ and v, (1.1) is equivalent to $\nabla r \cdot v = -\cos(\theta)$. Thus, the angle ∇r makes with unit vectors is also fixed by U_1.

Also, $||\nabla r|| < 1$ off edge points as U_1 is not tangent. By contrast, at an edge point, U and hence U_1 are tangent to M, so $||\nabla r|| = 1$ on edge points. This can only make correct sense at edge points if ∇r is computed using edge coordinates.

Remark 1.3. Often the Blum medial axis is approximated using triangular or rectangular pieces. The edges of these pieces are then included as part of the singular set of M. Hence, the compatibility condition must also be satisfied at these points in order to have smoothness of the boundary. The difficulty of obtaining smoothness is investigated in Yushkevich et al. (2002).

Finally, we mention that the Blum medial axis satisfies additional special properties not possessed by a general skeletal structure. These include : r being the same for all values of U at a given point, and at smooth points $x_0 \in M_{\text{reg}}$, the two values of U making equal angles with $T_{x_0}M$. We will find that these conditions are not crucial for understanding the geometry of the boundary.

2. Radial and Edge Shape Operators for 1D and 2D Medial Structures

2.1. Shape Operators and Principal Radial/Edge Curvatures

We begin by recalling from Damon (2003) the definition of the radial and edge shape operators as they apply to 1D and 2D medial axes.

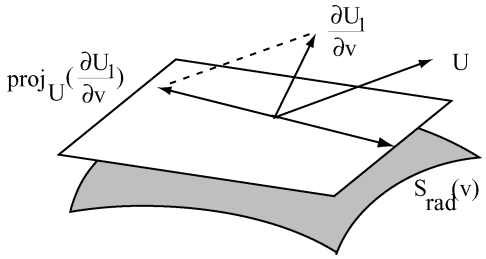

Figure 8. Projection for defining the radial shape operator. The dashed line denotes projection onto $T_{x_0}M$ along U.

2.2. Radial Shape Operator

Let (M, U) denote a Blum medial axis with radial vector field. Suppose we choose in a neighborhood of a non-edge point $x_0 \in M$, a smoothly defined value for U. Then, the radial shape operator (for this value of U) is defined for a tangent vector v to M at x_0 by

$$S_{\text{rad}}(v) = -\text{proj}_U\left(\frac{\partial U_1}{\partial v}\right)$$

with proj_U denoting projection onto the tangent space $T_{x_0}M$ along U (in general, this is not orthogonal projection, see Fig. 8). Unlike the differential geometric shape operator, S_{rad} is in general not symmetric. For a basis $\mathbf{v}$ of $T_{x_0}M$, we let $S_{\mathbf{v}}$ denote the matrix representation of S_{rad}. The *principal radial curvatures* and *principal radial directions* are the eigenvalues and eigendirections of S_{rad}.

Example 2.1. We first consider M a 1-dimensional Blum medial axis of an object in $\mathbb{R}^2$. If $\gamma(s)$ is a local parametrization of one of the smooth curve components of M, then write

$$\frac{\partial U_1}{\partial s} = a \cdot U_1 - \kappa_r \cdot \gamma'(s) \tag{2.1}$$

Then κ_r is principal radial curvature and the radial shape operator is then just multiplication by κ_r.

Example 2.2. Second, let M be a 2-dimensional Blum medial axis of an object in $\mathbb{R}^3$. Let $X(u_1, u_2)$ be a local parametrization of an open set W of one of the smooth sheets of M. Then, $v_i = \frac{\partial X}{\partial u_i}$, $i = 1, 2$ gives a basis for $T_{x_0}M$ at each point $x_0 \in W$. We write

$$\frac{\partial U_1}{\partial u_i} = a_i \cdot U_1 - b_{1i} \cdot v_1 - b_{2i} \cdot v_2 \quad i = 1, 2 \tag{2.2}$$

Then,

$$S_{\mathbf{v}} = \begin{pmatrix} b_{11} & b_{12} \\ b_{21} & b_{22} \end{pmatrix} \tag{2.3}$$

The principal radial curvatures are the two eigenvalues κ_{r1} and κ_{r2} of $S_{\mathbf{v}}$.

We remark that if we had used a different basis $\mathbf{w} = \{w_1, w_2\}$, then if C denotes the transformation for the change of basis from $\mathbf{v}$ to $\mathbf{w}$, then $S_{\mathbf{w}}, = CS_{\mathbf{v}}C^{-1}$.

2.3. Edge Shape Operator

Again we first give a dimension independent definition and then consider its meaning for 1D and 2D Blum medial axes. Let x_0 be an edge point, with a smooth value of U at x_0 corresponding to one side of M. Also, let n be a unit normal vector field to M pointing on the same side of M as a smooth value of U. We define

$$S_E(v) = -\text{proj}'\left(\frac{\partial U_1}{\partial v}\right)$$

Here proj′ denotes projection onto $T_{x_0}\partial M \oplus \langle \mathbf{n} \rangle$ along U (again generally this is not orthogonal, see Fig. 9).

We emphasize that $\frac{\partial U_1}{\partial v}$ has to be computed using edge coordinates. For $v \in T_{x_0}\partial M$, there is no problem, it is only for v pointing out from ∂M that we must be careful. For a matrix repesentation of S_E we use a special basis $\mathbf{v}$ for $T_{x_0}M$ consisting of a basis $\tilde{\mathbf{v}}$ for $T_{x_0}\partial M$ together with a vector in edge coordinates that maps to a multiple of $U_1(x_0)$. For $T_{x_0}\partial M \oplus \langle \mathbf{n} \rangle$ we use for a basis $\tilde{\mathbf{v}}$ and $\mathbf{n}$. We denote the matrix by $S_{E\mathbf{v}}$.

To define the principal edge curvatures, we let $I_{n-1,1}$ denote the $n \times n$-matrix obtained from the identity matix by changing the last entry to 0. For $n \times n$-matrices A and B, a generalized eigenvalue of (A, B)

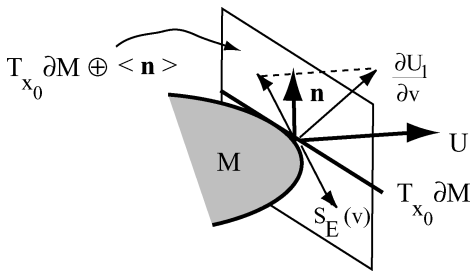

Figure 9. Defining the edge shape operator. The dashed line denotes projection onto $T_{x_0}M \oplus \langle \mathbf{n} \rangle$ along U.

is a λ such that $A - \lambda B$ is singular. The *principal edge curvatures* are defined to be the generalized eigenvalues Of $(S_{E\mathbf{v}}, I_{n-1,1})$.

Example 2.3. For a 1-dimensional Blum medial axis M of an object in $\mathbb{R}^2$, let $\gamma(s)$ be a local edge parametrization of M with say $\gamma(0) = x_0 \in \partial M$. Then, we write

$$\frac{\partial U_1}{\partial s} = a \cdot U_1 - c_{\mathbf{n}} \cdot \mathbf{n} \tag{2.4}$$

The edge shape operator is then multiplication by $c_{\mathbf{n}}$. As $I_{0,1}$ is the 1×1 0-matrix, provided $c_{\mathbf{n}} \neq 0$, there are no principal edge curvatures. Which is not surprising as the edge is 0-dimensional. The degenerate case would correspond to $c_{\mathbf{n}} = 0$, in which case all values are generalized eigenvalues. By Proposition 4.7 of Damon (2003), the Blum medial axis satisfies the edge condition (see Section 3), which implies that all positive generalized eigenvalues are bounded from below by $\frac{1}{r}$, a contradiction.

Example 2.4. For M a 2-dimensional Blum medial axis of an object in $\mathbb{R}^3$, we let $X(u_1, u_2)$ be a local edge parametrization of an open set W with $X(0, 0) = x_0 \in \partial M$. We suppose X chosen so that if $v_i = \frac{\partial X}{\partial u_i}, i = 1, 2$, then $v_1 \in T_{x_0}\partial M$ and v_2 maps under the edge parametrization to $c \cdot U_{1\tan}$, for $U_{1\tan}$ the tangential component of U_1 and $c \geq 0$. We write

$$\frac{\partial U_1}{\partial u_i} = a_i \cdot U_1 - c_{\mathbf{n}i} \cdot \mathbf{n} - b_i \cdot v_1 \quad 1 = l, 2 \tag{2.5}$$

Then, the edge shape operator has the matrix representation

$$S_{E\mathbf{v}} = \begin{pmatrix} b_1 & b_2 \\ c_{\mathbf{n}1} & c_{\mathbf{n}2} \end{pmatrix} \tag{2.6}$$

When $c_{\mathbf{n}2} \neq 0$, the single principal edge curvature is the generalized eigenvalue κ_E of $(S_{E\mathbf{v}}, I_{1,1})$ which we can compute as $\kappa_E = c_{\mathbf{n}2}^{-1} \cdot \det(S_{E\mathbf{v}})$. We shall explain in Proposition 3.7 how we may carry out computations while avoiding the use of edge coordinates.

2.4. *Conditions Implying the Smoothness of the Boundary*

Before stating how to use the radial and edge shape operators to compute the differential geometric shape operator, we first indicate a second important application

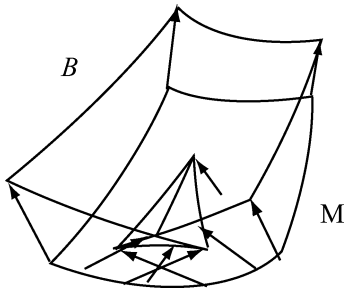

Figure 10. Singularities on a boundary associated to a skeletal structure.

of these operators. In the case that (M, U) is a skeletal structure, we can still ask when the associated boundary $\mathcal{B}$ is smooth. Figure 10 illustrates how the boundary associated to a skeletal structure may have singularities. We describe how we may ensure the smoothness of the associated boundary for general skeletal structures.

We define:

(1) (*Radial Curvature Condition*). For all points of M off ∂M
$r < \min\{\frac{1}{\kappa_{ri}}\}$ for all principal positive radial curvatures κ_{ri}
(2) (*Edge Condition*). For all points of $\overline{\partial M}$
$r < \min\{\frac{1}{\kappa_{Ei}}\}$ for all positive principal edge curvatures κ_{Ei}
(3) (*Compatibility Condition*). For all singular points of M (which includes edge points), $n_U \equiv 0$.

Then, the smoothness of the boundary is guaranteed by the following consequence of Damon (2003) Theorem 2.3.

Theorem 2.5. *Let (M, U) be a skeletal structure in $\mathbb{R}^2$ or $\mathbb{R}^3$ which satisfies: the Principal Curvature Condition, Edge Condition, and Compatibility Condition. Then,*

(i) *For M in $\mathbb{R}^2$, the associated boundary $\mathcal{B}$ is a C^1 curve which is smooth at all points corresponding to smooth points of M and which only has nonlocal intersections from distant points in M. If there are no nonlocal intersections then $\mathcal{B}$ is an embedded curve.*
(ii) *For M in $\mathbb{R}^3$:*
   (1) *the associated boundary $\mathcal{B}$ is an immersed surface which is smooth at all points except possibly at those corresponding to points of M_{sing}.*

(2) *At points corresponding to points of* M_{sing}, $\mathcal{B}$ *is weakly* C^1, *which means that it has a well defined limiting tangent space at such boundary points* (*this implies that it is* C^1 *except possibly at edge closure points*).
(3) *Also, if there are no nonlocal intersections,* $\mathcal{B}$ *will be an embedded surface.*

For both cases, at smooth points, the projection along the lines of U will locally map $\mathcal{B}$ *diffeomorphically onto the smooth part of M.*

Remark 2.6. In the case (M, U) is a Blum medial axis, Proposition 4.7 and Lemma 6.1 of Damon (2003) imply that (M, U) satisfies the radial curvature and edge conditions. Also, the compatibility condition will be satisfied at all points of M .

We also note that the radial curvature and edge conditions relate the pure radial distance information given by r with the pure radial direction information computed from U_1 (and in the Blum case the distance and direction properties are further related by the compatibility condition holding on all of M).

Example 2.7. For a 1-dimensional Blum medial axis M (or more generally a skeletal structure), by Example 2.1, the radial curvature condition becomes:

$$r < \frac{1}{\kappa_r} \quad \text{if } \kappa_r > 0, \text{ and no condition otherwise.}$$

The edge condition reduces to $c_{\mathbf{n}} \neq 0$ (otherwise all values are generalized eigenvalues). Finally, if $\gamma(s)$ is a unit speed parametrization of a smooth component of M with say $\gamma(0) = x_0 \in M$, then the compatibility condition becomes $U_1 \cdot \gamma'(0) + \frac{\partial r}{\partial s} = 0$. As x_0 approaches an edge point, the compatibility condition has limiting form $1 + \frac{\partial r}{\partial s} = 0$, which is a well-known property of the Blum medial axis. Here there is the proviso that the meaning of the derivative $\frac{\partial r}{\partial s}$ has to be reinterpreted using edge coordinates.

Example 2.8. For a 2-dimensional Blum medial axis M, by Example 2.2, the radial curvature condition becomes:

$$r < \min\left\{\frac{1}{\kappa_{ri}}\right\} \quad \text{for those } \kappa_{ri} > 0 \quad i = 1, 2.$$

The edge condition becomes by Example 2.4, for $\kappa_E = c_{n2}^{-1} \cdot \det(S_{E\mathbf{v}})$

$$r < \frac{1}{\kappa_E} \quad \text{if } \kappa_E > 0 \quad \text{otherwise no condition.}$$

For example, if both $\kappa_{ri} < 0$ then as we see in Section 4, the boundary is convex and there is no condition. If instead both $\kappa_{ri} > 0$ then (by Section 4) the boundary is concave and both κ_{ri} place restrictions on r.

3. Intrinsic Differential Geometry of the Boundary

3.1. Differential Geometric Shape Operator in terms of the Radial Shape Operator

We begin by expressing the differential geometric shape operator for the boundary $\mathcal{B}$ at a boundary point $x_0' \in \mathcal{B}$ associated to a non-edge point $x_0 \in M$. We let $\mathbf{v}'$ be the image under the radial map $d\psi_1$ of a basis $\mathbf{v} = \{v_1, \ldots, v_n\}$ of $T_{x_0}M$ (or for $T_{x_0}M_\alpha$ in case $x_0 \in M_{\text{sing}}$, where the value of U extends smoothly to the smooth sheet M_α). We can apply Theorem 3.2 of Damon to the special case of Blum medial axes.

Theorem 3.1. *Suppose* (M, U) *is a Blum medial axis with radial vector field. Let* $x_0' \in \mathcal{B}$ *correspond to the non-edge point* $x_0 \in M$ *as in the preceding situation.*

(1) *The differential geometric shape operator* $S_{\mathcal{B}}$ *of* $\mathcal{B}$ *at* x_0' *has a matrix representation with respect to* $\mathbf{v}'$ *given by*

$$S'_{\mathcal{B}\mathbf{v}} = (I - r \cdot S_{\mathbf{v}})^{-1} S_{\mathbf{v}} \tag{3.1}$$

(2) *There is a bijection between the principal curvatures* κ_i *of* $\mathcal{B}$ *at* x_0' *and the principal radial curvatures* κ_{ri} *of* M *at* x_0 (*counted with multiplicities*) *given by*

$$\kappa_i = \frac{\kappa_{ri}}{1 - r\kappa_{ri}} \quad \text{or equivalently } \kappa_{ri} = \frac{\kappa_i}{(1 - r\kappa_i)} \tag{3.2}$$

(3) *The principal radial directions corresponding to* κ_{ri} *are mapped by* $d\psi_1$ *to the principal directions corresponding to* κ_i.

Remark. A simpler way to express (3.2) is in terms of the signed radii of curvatures and radial curvatures, see Section 5. This alternate form immediately reveals the "relative nature" of comparing principal curvatures at distinct points using the relations (3.2).

Example 3.2. For a 1D Blum medial axis, we obtain that the curvature for the boundary curve $\mathcal{B}$ at a point

which corresponds to a non-edge point (and particular value of U) is given by

$$\kappa = \frac{\kappa_r}{1 - r\kappa_r}$$

Example 3.3. For a 2D Blum medial axis, the boundary points corresponding to edge points of M are crest points. For a non-crest point x_0' corresponding to a non-edge point x_0, we compute $S_{\mathbf{v}}$ as in (2.3) by the 2×2-matrix (b_{ij}). We obtain the principal radial curvatures and directions from the eigenvalues and eigenvectors of $S_{\mathbf{v}}$. Then, we obtain the principal curvatures of $\mathcal{B}$ by applying (3.2), and the principal directions by applying $d\psi_1$ to the eigenvectors. Finally, we obtain the matrix representation $S_{\mathcal{B}\mathbf{v}'}$ for the differential geometric shape operator by (3.1). In doing this, we determine the differential geometry using what is essentially the minimal amount of medial information possible (see also Section 6).

We also note that from $S_{\mathcal{B}\mathbf{v}'}$ we can easily compute the *Second Fundamental Form II* $(v_i', v_j') = v_i' \cdot S_{\mathcal{B}}(v_j')$. A matrix representation of II with respect to the basis $\mathbf{v}'$ is given by $G \cdot S_{\mathcal{B}\mathbf{v}'}$ where $G = (g_{ij})$ is given by the metric on $\mathcal{B}$ by $g_{ij} = v_i' \cdot v_j' \cdot G$ can be computed using $d\psi_i$ by Damon (2003), Section 4. However, it follows from the formula (3.1) that shape operators give the most direct relation between the differential geometry of $\mathcal{B}$ and medial data.

Next, we consider how the differential geometric shape operator at a crest point x_0' on $\mathcal{B}$ (corresponding to an edge point x_0 can be determined from the edge shape operator. For a special basis $\mathbf{v}$ at x_0 with corresponding basis $\mathbf{v}'$, we may apply [Damon (2004), Corollary 3.6].

Theorem 3.4. *Suppose (M, U) is a Blum medial axis and radial vector field of a region with smooth boundary. For a crest point x_0' on $\mathcal{B}$ corresponding to an edge point x_0 as above, the differential geometric shape operator for $\mathcal{B}$ at x_0' has a matrix representation with respect to $\mathbf{v}'$ given in terms of the edge shape operator by*

$$S_{\mathcal{B}\mathbf{v}'} = (I_{n-1,1} - r \cdot S_{E\mathbf{v}})^{-1} S_{E\mathbf{v}} \tag{3.3}$$

Hence, the principal curvatures κ_i and principal directions of $\mathcal{B}$ at x_0' are the eigenvalues and eigendirections (after identification by $d\psi_1$) of the RHS of (3.3).

Example 3.5. For a 1D Blum medial axis, at a point of the boundary curve $\mathcal{B}$ corresponding to an edge point, we obtain from (3.3) that

$$\kappa = (0 - rc_{\mathbf{n}})^{-1} c_{\mathbf{n}} = \frac{-1}{r}.$$

This is the curvature of the osculating circle of radius r (with minus sign resulting from an outward pointing normal vector).

Example 3.6. For a 2D Blum medial axis, at a crest point of the boundary surface $\mathcal{B}$, we computed the edge shape operator in Example 2.4. Thus, by (3.3) we compute the differential geometric shape operator. Let $K_E = \det(S_{E\mathbf{v}})$. Then,

$$\begin{aligned} S_{\mathcal{B}_{\mathbf{v}'}} &= \begin{pmatrix} 1 - rb_1 & -rb_2 \\ -rc_{\mathbf{n}1} & -rc_{\mathbf{n}2} \end{pmatrix}^{-1} \begin{pmatrix} b_1 & b_2 \\ c_{\mathbf{n}1} & c_{\mathbf{n}2} \end{pmatrix} \\ &= \begin{pmatrix} \frac{K_E}{c_{\mathbf{n}2} - rK_E} & 0 \\ \frac{c_{\mathbf{n}1}}{r(rK_E - c_{\mathbf{n}1})} & -\frac{1}{r} \end{pmatrix} \end{aligned} \tag{3.4}$$

Hence, we see that

$$\text{the principal curvatures are: } -\frac{1}{r} \quad \text{and} \quad \frac{K_E}{c_{\mathbf{n}2} - rK_E} \tag{3.5}$$

We note the special case where $\frac{\partial U_1}{\partial v_1}$ is orthogonal to $\mathbf{n}$. This implies $c_{\mathbf{n}1} = 0$, so in (3.4) $K_E = b_1 c_{\mathbf{n}2}$. Then, by (3.4), $S_{\mathcal{B}\mathbf{v}'}$ becomes diagonal with eigenvalues $\frac{1}{\frac{1}{b_1} - r}$ and $-\frac{1}{r}$.

To compute the differential geometric shape operator at a crest point, we must use edge coordinates, which we are not a priori given. A way around this is to compute $S_{\mathcal{B}\mathbf{v}'}$ as a limiting value. We let v_1 be a smooth vector field on a neighborhood W of the edge point x_0 which is tangent to ∂M. Here smoothness is only in the sense of a surface with edge. We also let $v_2 = U_{1\tan}$ the tangential component of U_1. Then, both $U_{1\tan}$ and v_1 are smooth for edge coordinates. Then, we can compute at smooth points $x \in W$ near x_0, a related operator S_E' extending S_E as follows.

$$S_E'(v) = -\text{proj}_U'' \left(\frac{\partial U_1}{\partial v} \right) \tag{3.6}$$

where now proj_U'' denotes projection along U but onto L, the subspace spanned by $\{v_1, \mathbf{n}\}$. Then, we apply Proposition 3.9 of Damon (2004) to conclude.

Proposition 3.7. *In the preceding situation $S_{\mathcal{B}\mathbf{v}'}$ the differential geometric shape operator at a crest point x_0', with respect to the basis $\mathbf{v}'$ associated to $\mathbf{v}$ is given by*

$$S_{\mathcal{B}\mathbf{v}'} = \lim_{x \to x_0} (I_{1,1} - r \cdot S'_{E\mathbf{v}}) \tag{3.7}$$

Hence, the principal curvatures at x_0' are the limits as $x \to x_0$ of the eigenvalues of the RHS of (3.7)*. Moreover, if the principal curvatures at x_0 are distinct, then the principal directions are the limits of the eigendirections of the RHS of* (3.7) *as $x \to x_0$.*

Although computationally we cannot really take a limit as in Proposition 3.7, by choosing x sufficiently close to x_0, we can compute the RHS of (3.7) to determine good approximations to both the eigenvectors and eigenvalues for the crest point x_0'.

3.2. Geometry in the Non-Blum Case

To express the differential geometric shape operator of the boundary in the non-Blum case requires in addition to S_{rad} both η_U and its first derivatives. We do not explicitly give the formula here. However, suppose that (M, U) is "almost Blum" , which means that although η_U is not identically zero on M, both η_U and its first derivatives are small. For the Blum case, $\eta_U \equiv 0$ on the smooth points. This doesn't hold exactly in concrete situations; however, if η_U is close to zero then U_1 will be approximately the normal vector. If in addition, the derivatives of η_U are small then the variation of U_1 will closely approximate the variation of the normal vector to the boundary. Then, the formulas in Theorems 3.1 and 3.4 will approximately give the correct differential geometric shape operator. Hence, since S_{rad} is as easy to compute in the non-Blum case as in the Blum case, we are able to approximately determine the geometry of the boundary in the "almost Blum case". We shall see in the next sections this has further consequences for constructing a geometric medial map in the almost Blum case which approximately determines the intrinsic and relative geometry of the associated boundary.

4. Intrinsic Part of the Geometric Medial Map

In the preceding section, we explicitly expressed the differential geometric shape operator in terms of the radial or edge shape operators by formulas which also involved r. We go further in this section to construct the portion of the geometric medial map which is defined solely in terms of the radial shape operator to construct geometric objects on the medial axis which correspond under the radial map to the corresponding objects for the differential geometry of the associated boundary $\mathcal{B}$.

In light of the results from the preceding section, it is sufficient to establish the following.

Lemma 4.1. *Suppose (M, U) is a Blum medial axis of a region Ω with smooth boundary $\mathcal{B}$. Let $x_0 \in M$ be a smooth point with associated point $x_0' \in \mathcal{B}$. Under the correspondence* (3.2)*, the principal radial curvatures at x_0 have the same sign as the corresponding principal curvatures at x_0' and one is zero iff the other is.*

Proof: By Proposition 4.7 of Damon (2003), (M, U) satisfies the radial curvature condition at all smooth points of M. Thus, $r < \min\{\frac{1}{\kappa_{ri}}\}$ for all $\kappa_{ri} > 0$. First, from (3.2) it immediately follows that $\kappa_{ri} = 0$ iff $\kappa_i = 0$.

Second, if both are nonzero, suppose first $\kappa_{ri} < 0$. Then, $1 - r\kappa_{ri} > 0$; and hence by (3.2) $\kappa_i < 0$. If instead $\kappa_{ri} > 0$, then by the radial curvature condition $1 - r\kappa_{ri} > 0$ so by (3.2) $\kappa_i > 0$. □

Given the Blum medial axis M of a region Ω with smooth boundary $\mathcal{B}$, we can use S_{rad} to define on M_{reg} the "radial analogues" of the corresponding objects for classical differential geometry of surfaces. For example, $K_r = \det(S_{\text{rad}})$ is the radial curvature; the curve where $\det(S_{\text{rad}}) = 0$ is the radial parabolic curve; etc. Define the intrinsic part of the *geometric medial map* to consist of the radial versions of geometric objects given in the left hand column of Table 1. Then the relation between the two columns of Table 1 is provided by the radial map ψ_1.

Table 1. Intrinsic part of geometric medial map.

Radial shape operator	$\overset{\psi_1}{\Longleftrightarrow}$	Differential geometry of boundary
Relation between geometric medial map and differential geometry of the boundary		
(i) Regions of positive (negative) radial curvature		(i) Regions of positive (negative) Gaussian curvature
(ii) Parabolic radial curves		(ii) Parabolic curves
(iii) Radial umbilic points		(iii) Umbilic points
(iv) Signs of principal radial curvatures		(iv) Signs of principal curvatures
(v) Principal radial directions		(v) Principal directions
(vi) Principal radial curves		(vi) Principal curves

Theorem 4.2. *For the Blum medial axis (M, U) of a region Ω with smooth boundary $\mathcal{B}$, the radial map sends the radial objects in the geometric medial map (in the first column of Table 1) to the corresponding differential geometric objects for $\mathcal{B}$ in the second column of Table 1.*

Proof: First, by Lemma 4.1, the sign of a principal curvature κ_i agrees with that of the corresponding principal radial curvature κ_{ri}; and $\kappa_r = 0$ iff $\kappa_{ri} = 0$. Hence, for a point $x_0' \in \mathcal{B}$ which corresponds to $x_0 \in M_{\text{reg}}$ via the radial map, any property at x_0' which can be given in terms of the signs of the principal curvatures can be expressed in terms of the same conditions for the signs of the corresponding principal radial curvatures. In particular the correspondence in Table 1 involving (i), (ii) and (iv) follows. For (iii) we use the formulas in (3.2) relating κ_i and κ_{ri}. Since the same r is used at a point, $\kappa_1 = \kappa_2$ iff $\kappa_{r1} = \kappa_{r2}$.

Lastly, by Theorem 3.1, $d\psi_1$ sends the principal radial directions to principal directions giving $\mathbf{v}$), and hence a principal radial curve will map by ψ_1 to a curve whose tangent lines are principal directions, and so is a principal curve. □

In Fig. 11, we see that distinct properties of boundaries can be detected by the intrinsic part of the geometric medial map.

5. Intrinsic versus Relative Geometry of the Boundary

To understand the role of r for the relative geometry of the boundary B,we begin by considering how we compare the values of principal curvatures at different points of $\mathcal{B}$ in terms of medial data. To compare their values, we consider the *signed radii of curvature* $r_i \stackrel{\text{def}}{=} \frac{1}{\kappa_i}$ and the corresponding *signed radii of radial curvature* $r_{ri} \stackrel{\text{def}}{=} \frac{1}{\kappa_{ri}}$. We note that in terms of the signed curvatures, (3.2) can be rewritten in the following *radii of curvature equation*:

$$r_{ri} = r + r_i \quad \text{for all } i \tag{5.1}$$

We next see this gives us an immediate comparison of principal curvatures at distinct points in terms of medial data. Consider two points x_0' and x_1' in $\mathcal{B}$ which correspond to points $x_0, x_1 \in M_{\text{reg}}$ and a smooth value of U defined at both points (so x_0' and x_1' lie on the same side of the smooth sheet of M). We let κ_i be a principal curvature at x_0' with κ_{ri} the corresponding principal radial curvature at x_0 and let r be the radial function. For x_1' we add primes to denote the corresponding objects, e.g. κ_i' will be the corresponding principal curvature at x_1', etc. To compare κ_i and κ_i', we suppose they have the same sign (otherwise we can use Theorem 4.2 to distinguish which is larger).

Proposition 5.1. *If κ_i and κ_i' have the same sign, then*

$$\kappa_i < \kappa_i' \quad \textit{iff} \quad r - \frac{1}{\kappa_{ri}} < r' - \frac{1}{\kappa_{ri}'} \tag{5.2}$$

In particular, if $\kappa_{ri} < \kappa_{ri}'$ and $r \le r'$, then $\kappa_i < \kappa_i'$.

Proof: Let r_i and r_i' denote the corresponding signed radii of curvatures. As κ_i and κ_i' have the same sign, $\kappa_i < \kappa_i'$ iff $r_i > r_i'$. Then, by (5.1), this is equivalent to $r_{ri} - r > r_{ri}' - r'$, and hence to $r - \frac{1}{\kappa_{ri}} < r' - \frac{1}{\kappa_{ri}'}$. Thus, if $\kappa_{ri} < \kappa_{ri}'$ then $\frac{1}{\kappa_{ri}} > \frac{1}{\kappa_{ri}'}$. Together with $r \le r'$, this implies the right hand inequality in (5.2). □

A second consequence of (5.1) is to identify critical points of κ_i along curves in $\mathcal{B}$. A critical point x_0' of κ_i along a curve $\gamma_1(s)$ is also a critical point for r_i (provided $\kappa_i \neq 0$). Suppose γ_1 is the image of γ under ψ_1 with $x_0' = \psi_1(x_0)$ Then, by (5.1), $\frac{\partial r_i}{\partial s} = 0$ iff $\frac{\partial r_{ri}}{\partial s} = \frac{\partial r}{\partial s}$. Thus, we summarize.

Corollary 5.2. *In the preceding situation, a critical point $x_0' = \psi(x_0)$ of κ_i along a curve $\gamma_1 = \psi \circ \gamma$ corresponds to the point x_0 where $\frac{\partial r_{ri}}{\partial s} = \frac{\partial r}{\partial s}$.*

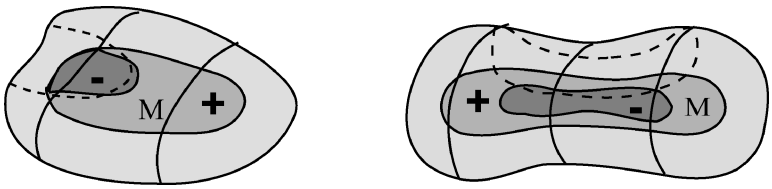

Figure 11. Illustrating geometric medial maps capturing distinct properties of boundaries (in this case regions where gaussian curvature changes sign).

The preceding is relevant for various "ridges of principal curvature" considered by Bruce et al. (1996). One such is the crest curve, which corresponds to the edge of the medial axis. However, there are other ridge-type curves and these can be identified from medial data using the principal radial curvatures and radial function. As explained in Bruce et al. (1996), these ridge-type curves concern the geometry of $\mathcal{B}$ as an embedded surface. This is distinct from the relative geometry of $\mathcal{B}$ as the boundary of an object. We next introduce a method for analyzing this geometry.

Remark 5.3. Suppose (M, U) is partially Blum satisfying the radial, edge, and compatibility conditions. The associated boundary will be smooth in the sense of Theorem 2.5. The spheres of radius r at points M will be tangent to the associated boundary; however, they may not lie entirely in the region. As observed by Tom Fletcher, we may ensure the spheres are within the boundary, at least locally in a neighborhood of the points of tangency, by requiring that $r < |r_i|$ for all principal radii $r_i < 0$. We claim this is guaranteed by the radial curvature condition together with the radii of curvature equation (5.1). To see this we note that if $r_i < 0$, then by (5.1) $r < |r_i|$ iff $r_{ri} < 0$. However, if $r_{ri} > 0$, then by Lemma 4.1, $r_{ri} > 0$, a contradiction.

6. Relative Geometry of the Boundary via Relative Critical Sets

We saw in the previous section that r plays an important role in the relative geometry of the boundary when we compare geometry at distinct points of the boundary in terms of medial data. We now turn more generally to the relative geometry as captured by properties of r on the medial axis. To capture such relative geometry we use the "relative critical set of r".

We first recall how the relative critical set captures geometry of a function f on $\mathbb{R}^2$, and then explain how it extends to r on the medial axis.

6.1. *Relative Critical Sets on* $\mathbb{R}^2$

Consider a smooth function $f\colon W \to \mathbb{R}$, for W an open subset of $\mathbb{R}^2$. For a point $x_0 \in W$, let $\lambda_1 < \lambda_2$ denote the eigenvalues of the Hessian $H(f)(x_0)$, with eigenvectors e_1 and e_2. First, x_0 is called a (*height*) *ridge point* of f if $\nabla f(x_0)$ is orthogonal to e_1 and $\lambda_1 < 0$. The (height) ridge, which we henceforth call the ridge of f, is the set of (height) ridge points of f. A ridge curve represents the points along which the function is decreasing most rapidly in the directions orthogonal to the gradient direction. It was introduce by Pizer and Eberly to investigate properties of gray-scale "medial functions" (Pizer et al., 1998; Eberly, 1996). The ridge will generally consist of pieces of smooth curves. These curves carry information about the graph of f, viewed as a surface, but where the direction of the dependent variable remains distinguished.

However, the ridge curves consist of disjoint pieces without any structure to relate them. This is because they are only part of the complete structure needed to reveal the full geometry of f. This structure is called the *relative critical set of* f. We consider in addition to the ridge set the following sets of points consisting of those x_0 which are:

1. *valley points* for which $\nabla f(x_0)$ is orthogonal to e_2 and $\lambda_2 > 0$,
2. *r-connector points* for which $\nabla f(x_0)$ is orthogonal to e_1 and $\lambda_1 > 0$, and
3. *v-connector points* for which $\nabla f(x_0)$ is orthogonal to e_2 and $\lambda_2 < 0$.

Then, the relative critical set, denoted $\mathcal{RC}(f)$ is the closure of the four ridge, valley, r-connector, and v-connector sets. In addition, it contains: critical points, singular Hessian points (where one of the $\lambda_i = 0$), and (partial) umbilic points (where $\lambda_1 = \lambda_2$). For higher dimensions one can analogously define relative critical sets, except they become increasingly more varied as the dimension increases (see Damon, 1998, 1999; Miller, 1998; Keller, 1999). As an example of a relative critical set for a function, see Fig. 12 which exhibits ridge and valley curves and v-connector curves.

Remark 6.1. For generic f on $\mathbb{R}^2$, the relative critical set has the following generic properties: each of the four types form smooth curves; these curves only cross at critical points which are nondegenerate; the types of curves which can cross are determined by the type of the critical point (see Fig. 13); the curves can change from one type to another as they pass through singular Hessian or (partial) umbilic points; and the specific changes are uniquely determined (see Fig. 14). This network of curves does not end (as e.g. Blum medial axes do) but continues to the end of the open set.

Furthermore, they satisfy stability properties under perturbation of f (Damon, 1998) and generic

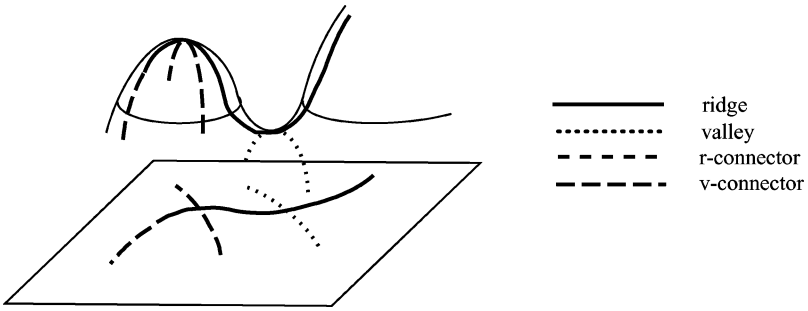

Figure 12. Graph of a function, with the relative critical set exhibiting ridge, valley, and v-connector curves, with the corresponding curves on the graph.

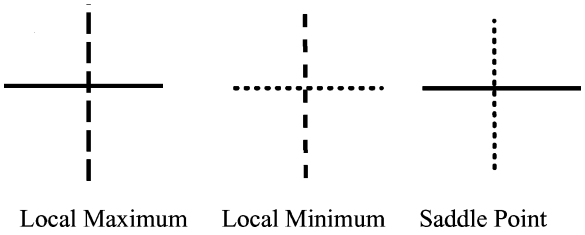

Figure 13. Crossings of relative critical set curves at critical points.

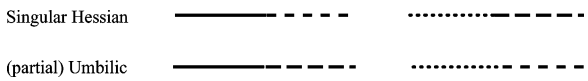

Figure 14. Changing type for relative critical set at singular Hessian and (partial) Umbilic points.

transitions which can occur in one parameter families are also determined (Damon, 1998; Keller, 1999).

6.2. *Relative Critical Sets for Functions on Surfaces*

We wish to extend the preceding to r on the medial axis. As an intermediate step, we consider a function $f : N \to \mathbb{R}$ where N is a smooth surface (in $\mathbb{R}^3$). N is a special case of a Riemannian manifold and the dot product on the tangent space of N is denoted $\langle , \rangle$. Eberly (1996) used generalized eigenvalues and tensor index notation to define the (height) ridge of f on any Riemannian manifold. We are going to give a formulation of the relative critical set for f which for the ridge part will be equivalent to that given by Eberly.

We let ∇f be the Riemannian gradient so that $< \nabla f, v >= df(v)$. Then, ∇f is a vector field on N which is orthogonal to the level curves of f on N. Also, the Riemannian Hessian is defined by $H(f)(v, w) \stackrel{\text{def}}{=} < \nabla_v(\nabla f), w >$. Here "$\nabla_v$" denotes the covariant derivative of the vector field ∇f (we note that $\nabla_v X(x_0) = \text{proj}_{\mathbf{n}}(\frac{\partial X}{\partial v})$ for a vector field X, where $\text{proj}_{\mathbf{n}}$ denotes orthogonal projection onto $T_{X_0}N$). By properties of the covariant derivative, $H(f)$ is symmetric in v and w. We define the Hessian operator $H_f : T_{x_0}N \to T_{x_0}N$ by $H_f(v) = \nabla_v(\nabla f)$. As $< H_f(v), w >= H(f)(v, w)$, it follows that H_f is self-adjoint, and so it has real eigenvalues, and the eigenvectors for distinct values are orthogonal.

We again let $\lambda_1 < \lambda_2$ denote the eigenvalues of the Hessian operator H_f at x_0, with eigenvectors e_1 and e_2. Then, we repeat the definition for ridge, valley, r-connector, and v-connector sets. It is shown in Damon (in preparation) that the same generic properties for functions on $\mathbb{R}^2$ which we listed in Remark 6.1 continue to hold for generic smooth functions on a given smooth surface N. This brings us to the case of r on the medial axis M.

6.3. *Relative Geometry in the Non-Blum Case*

If (M, U) is a general skeletal structure, then M is a stratified set. We can consider the relative critical set of r on M_{reg}. In the general case r need not be the same for each side of M. Hence, for each side of each smooth sheet of M_{reg}, the relative critical set $\mathcal{R}C(r)$ is a network of curves which generically will have the properties in Remark 6.1. Here by genericity, we mean that given a compact subset C of M_{reg} there is an open dense set of smooth functions on M, for which the relative critical sets exhibit the generic properties on C. Genericity holds even for skeletal structures (M, U) satisfying the radial curvature, edge and compatibility conditions, as will follow from Theorem 6.4. The ridge curve will be a ridge of thickness; the valley curve will be a valley of thinness. Along the r-connector curve, the gradient points in the direction of "greatest increase"; and along the v-connector curve, the gradient points in the direction of "greatest decrease". Without the compatibility

condition on all of M there is no real condition on U_1. This is remedied in the Blum case.

6.4. *Relative Part of the Geometric Medial Map on the Blum Medial Axis*

We now consider a Blum medial axis M and radial vector field (M, U) for a region Ω with smooth boundary $\mathcal{B}$. M will still in general be a stratified set instead of a smooth surface. The compatibility condition places restrictions on r so it is not an arbitrary function even on M_{reg}. We need to deal with both of these questions as well as use the compatibility condition to give more explicit criteria for belonging to the various parts of the relative critical set.

First by the compatibility condition, $\nabla r = -U_{1\tan}$, the tangential component of U_1. Thus, the Hessian operator for r takes the form $H_r(v) = -\nabla_v U_{1\tan}$. Thus, $\nabla r = -U_{1\tan}$ being orthogonal to an eigenvector e_i is equivalent to $U_{1\tan}$ being an eigenvector (a multiple of e_j), with eigenvalue $\lambda(=\lambda_j)$ for H_r. Hence we have the following description of the relative critical set of r on M_{reg} using only $U_{1\tan}$.

Proposition 6.2. *Suppose (M, U) is a Blum medial axis and radial vector field for a region with smooth boundary $\mathcal{B}$. The relative critical set of r on M_{reg} consists of those $x_0 \in M_{\text{reg}}$ such that*

$$-\nabla_{U_{1\tan}}(U_{1\tan}) = \lambda \cdot U_{1\tan} \tag{6.1}$$

If μ is the other eigenvalue of $H_r(v) = -\nabla_v U_{1\tan}$, then the different types of points are characterized as follows:

(1) *for ridge points $\mu < 0$ and $\mu < \lambda$;*
(2) *for valley points $\mu > 0$ and $\mu > \lambda$;*
(3) *for r-connector points $\mu > 0$ and $\mu < \lambda$; and*
(4) *for v-connector points $\mu < 0$ and $\mu > \lambda$.*

The earlier Fig. 4 illustrates the relative critical set of the radial function on the Blum medial axis.

To state what genericity means in this case, we consider Blum medial axes and radial vector fields (M, U) with M fixed.

Definition 6.3. By a multivalued vector field U (and r) being *allowable* for M we mean that (M, U) is a Blum medial axis of a region with smooth boundary.

Then, by *genericity of a property for Blum medial axes,* we mean that for a fixed M, given a compact subset C of M_{reg}, there is an open dense subset of allowable U such that (M, U) exhibits the property on C.

We then can state the genericity of properties of the relative critical set of r for Blum medial axes.

Theorem 6.4. *For Blum medial axes, the relative critical set of a generic r possesses the same generic properties (on a compact subset C of M_{reg}) as functions on $\mathbb{R}^2$.*

Remark. Since for genericity we may choose as large a compact subset of M_{reg} as we desire, the conditions will hold off as small a neighborhood of M_{sing} as we wish. The argument we give will also apply to a skeletal set (possibly satisfying the three conditions). With a more careful analysis it should be possible to state a form of genericity which holds on all of M.

Proof: Given the compact subset $C \subset M_{\text{reg}}$, we may choose an open neighborhood W of C in M_{reg}. Then, given U, and hence r, we can vary r to r' within a C^2 neighborhood of r on C and unchanged outside a compact subset of W containing C. Then, as (M, U) is a Blum medial axis, the original r satisfies the radial curvature conditions on W. Given the perturbed r', an associated radial vector field U' is determined by $U'_{1\tan} = -\nabla r'$ and $||U'_1|| = 1$ with U' pointing on each side of W.

First, as $r' = r$ off a compact subset of W, all conditions are satisfied off this compact subset. On W, by construction U' satisfies the compatibility condition.

Also, for r' sufficient close to r in the C^2 sense, then U' will satisfy the (open) radial curvature condition on W. Thus, all conditions for smoothness of the boundary are satisfied and because the original boundary was smooth, the new boundary will be smooth in a neighborhood of the image of M_{sing}, as it remains unchanged. Finally, for r' sufficiently close to r, the radial map remains one–one. Thus, the perturbation r' corresponds to a Blum medial axis (M, U') of a region with smooth boundary. Then, as we vary r within the C^2 neighborhood, we obtain a relative critical set with generic properties on C for an open dense subset of this C^2 neighborhood. This establishes the genericity. □

7. Radial versus Differential Geometry of the Medial Axis

We contrast the results on the geometry of the boundary we have obtained in earlier sections using the radial shape operator with the possible alternate approach using the differential geometry of the medial axis. As already mentioned the results previously obtained actually apply to the geometry of parallel surfaces of the boundary. One way to actually obtain results about the boundary itself would be to give a relation between the radial shape operator S_{rad} with the differential geometric shape operator S_{med} for the medial axis (at smooth points). As the derivatives of r must enter into any such relation, it is not surprising that the radial Hessian operator is involved. There is yet one other operator which must be included in the relation. We let $U_1 = \rho \text{n} + U_{1\tan}$ denote the decomposition of U_1 into normal and tangential components. Then, we define

$$Z(v) = \rho^{-l}\left(\frac{\partial U_1}{\partial v} \cdot \text{n}\right) U_{1\tan} \tag{7.1}$$

Z does not have an obvious geometric meaning. Also, in contrast to S_{med} and H_r, Z need not be self–adjoint. However, Z as well as H_r enter into the relation between the radial and the differential geometric shape operators for the medial axis (see Damon, 2004, Proposition 4.1).

Proposition 7.1. *Let (M, U) be a the Blum medial axis and radial vector field for a region with smooth boundary in $\mathbb{R}^{n+l}$. Then,*

$$S_{\text{rad}} = \rho \cdot S_{\text{med}} + H_r + Z. \tag{7.2}$$

If we combine this proposition with Theorem 3.1, we can express the differential geometric shape operator of the boundary in terms of S_{med} by substituting the expression for S_{rad} from (7.2) into (3.1). While the resulting expression will involve H_r as is expected, it will also involve Z. Thus, barring some remarkable unexpected identities, the representation in this form will be considerably more complicated than that in terms of S_{rad}.

8. Effects of Diffeomorphisms of a Skeletal Structures on the Smoothness and Geometry of Associated Boundary

One of the goals proposed by Stephen Pizer is to be able to perform operations on the medial axis and determine the effect on the resulting associated boundary. The approach we have developed only requires that the the effect be determined on the radial and edge shape operators and the compatibility 1-form. We demonstrate how such effects can be computed in the case a Blum medial axis is distorted or deformed by applying a diffeomorphism to it, as in Fig. 15.

Let (M, U) be the Blum medial axis and radial vector field associated to a region Ω with smooth boundary $\mathcal{B}$. We let $\mathcal{W}$ denote some arbitrarily small neighborhood of M, and let $\varphi : \mathcal{W} \to \mathbb{R}^{n+1}$ denote a diffeomorphism onto an open subset of $\mathbb{R}^{n+1}$. We then obtain $M' = \varphi(M)$ and $V = d\varphi(U)$. In general, (M', V) is not the Blum medial axis of a region. In fact, the associated boundary $\mathcal{B}'$ need not be smooth, nor even if it is, must M' be the Blum medial axis of the region it bounds. It is also not clear what new geometric properties $\mathcal{B}'$ will possess.

However, by the results we have described in earlier sections, we can give an answer to the preceding questions provided we can determine the radial and edge shape operators and the compatibility 1-form of (M', V). We explain how to do this in terms of the medial data of (M, U) together with certain "distortion operators". In this the differentiable structure of the medial axis does not change, but it should be possible to eventually include the generic changes in the medial axis using Bruce and Giblin (1986) and Bogaevski (2002).

8.1. Effects of Diffeomorphisms on Compatibility Conditions

We first describe the effects of φ on compatibility conditions. In general there are not simple sufficient

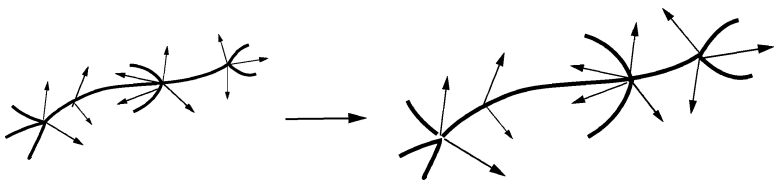

Figure 15. Example of a diffeomorphism of a skeletal structure.

conditions to ensure that (M', V) satisfy the compatibility conditions without a restriction on φ. We write $V = r_1 V_1$ where V_1 is the unit radial vector field. Also, we write $V_1 = \sigma d\varphi(U_1)$. We refer to σ as the *radial scaling factor.* We say that φ is *radially rigid on M* if $d\varphi(U_1) \cdot d\varphi(v) = U_1 \cdot v$ for all points in M and all $v \in \mathbb{R}^{n+1}$. It then follows that $||d\varphi(U_1)|| = ||U_1||$ so $\sigma \equiv 1$ (and $d\sigma \equiv 0$).

For example, if U is a normal vector field on an open subset of a smooth sheet of M, then the compatibility condition implies that r is constant on that subset so that portion of the boundary is a parallel surface (or curve in the 1D case). Under a radially rigid diffeomorphism, V will also be a constant length normal vector field on the image of that region, and the new associated boundary will also be a parallel surface (curve). However, otherwise we are free to deform the shape of M (provided the new boundary remains smooth).

The general relation is given by the following Lemma (see Damon (2004), Lemma 4.3).

Lemma 8.1. *If φ is radially rigid then, $\varphi^*(\eta_V) = \eta_U$ (or alternately $\varphi_*(\eta_U) = (\eta_V)$. Hence, if (M, U) satisfies the compatibility condition, then so does (M', V).*

Thus, a condition such as radial rigidity is first needed to ensure that (M', V) satisfies the compatibility condition for being a Blum medial axis. However, just to ensure that $\mathcal{B}'$ is smooth, it is only necessary to have the compatibility condition hold on M'_{sing} which will follow from radial rigidity on M_{sing} (again see the more detailed [Damon (to appear), Lemma 4.3]).

8.2. Radial and Edge Distortion Operators

To determine the effects of φ on the radial and edge shape operators, we introduce corresponding distortion operators. These involve the second derivative of φ.

8.2.1. Radial Distortion Operator. For a nonedge point x_0, we define the radial distortion operator Q_φ for $v \in T_{x_0}M$ by

$$Q_\varphi(v) = -d\varphi^{-1}(\text{proj}_V(d^2\varphi_{x_0}(v, U_1))) \quad (8.1)$$

We give a matrix representation of this operator in the 1D and 2D cases.

Example 8.2 (Radial Distortion Operators for 1D and 2D Medial Axes). For a 1D medial axis M, let $\gamma(s)$ denote a parametrization of a smooth component of M with say $x_0 = \gamma(0)$. Then, $\gamma_1 = \varphi \circ \gamma$ is a parametrization of M' near $x'_0 = \varphi(x_0)$. We write

$$d^2\varphi_{x_0}(\gamma'(0), U_1) = a_1 \cdot V_1 - q \cdot \gamma'_1(0) \quad (8.2)$$

Then, Q_φ is multiplication by q.

For a 2D medial axis M, let $X(u_1, u_2)$ denote a parametrization of a smooth component of M with say $x_0 = X(0, 0)$. Then, $X_1(u_1, u_2) = \varphi \circ X(u_1, u_2)$ is a parametrization of M' near $x'_0 = \varphi(x_0)$. As in Example 2.2, we let $v_i = \frac{\partial X}{\partial u_i}$, $i = 1, 2$ denote a basis for $T_{x_0}M$ at each point x_0 in the parametrized region. We write

$$d^2\varphi_{x_0}(v_i, U_1) = a_i \cdot V_1 - q_{1i} \cdot v'_1 - q_{2i} \cdot v'_2 \quad i = 1, 2 \quad (8.3)$$

where $v'_i = d\varphi(v_i) = \frac{\partial X_1}{\partial u_i}$. Then, $Q_{\varphi \mathbf{v}}$, the matrix representation of Q_φ with respect to the basis $\mathbf{v} = \{v_1, v_2\}$ is given by

$$Q_{\varphi \mathbf{v}} = \begin{pmatrix} q_{11} & q_{12} \\ q_{21} & q_{22} \end{pmatrix} \quad (8.4)$$

8.2.2. Edge Distortion Operators. Next, we consider the effect of φ on edge shape operators. We really only need consider the 2D case, for in the 1D case the radius of curvature in the Blum case will be $-\frac{1}{r_1}$. Let x_0 be an edge point (or we consider a local edge manifold component for an edge closure point). We define the edge distortion operator $Q_{E,\varphi}$ by

$$Q_{E,\varphi}(v) = -d\varphi^{-1}(\text{proj}'_{\mathbf{v}}(d^2\varphi_{x_0}(v, U_1))) \quad (8.5)$$

We give a matrix representation of this operator in the 2D case.

Example 8.3 (Edge Distortion Operators for 2D Medial Axes). We let v_1 be a smooth vector field tangent to ∂M, and let $v_2 = U_{1\tan}$ We again let $v'_i = d\varphi(v_i)$. Then, we write

$$d^2\varphi_{x_0}(v_i, U_1) = a'_i \cdot V_1 - c_i \cdot n - \tilde{q}_i \cdot v'_1 \quad i = 1, 2 \quad (8.6)$$

Then, the matrix representation $Q_{E\varphi,\mathbf{v}}$ of $Q_{E,\varphi}$ is given by

$$Q_{E\varphi,\mathbf{v}} = \begin{pmatrix} \tilde{q}_1 & \tilde{q}_2 \\ c_1 & c_2 \end{pmatrix} \quad (8.7)$$

In addition we must also take into account the failure of $d\varphi$ to send $\mathbf{n}$ to $\mathbf{n}'$ at edge points of M. We write

$$d\varphi_{x_0}(\mathbf{n}) = a_{\mathbf{n}} \cdot V_1 + c_{\mathbf{n}} \cdot \mathbf{n}' + b_{\mathbf{n}} \cdot v_1' \tag{8.8}$$

Then, we define

$$E_{\varphi \mathbf{v}} = \begin{pmatrix} c_{\mathbf{n}1} b_{\mathbf{n}} & c_{\mathbf{n}2} b_{\mathbf{n}} \\ c_{\mathbf{n}1}(c_{\mathbf{n}} - 1) & c_{\mathbf{n}2}(c_{\mathbf{n}} - 1) \end{pmatrix} \tag{8.9}$$

where $c_{\mathbf{n}i}$ are defined in (2.5). We observe that if $d\varphi(\mathbf{n}) = \mathbf{n}'$, then $c_{\mathbf{n}} = 1$ and $b_{\mathbf{n}} = 0$ so $E_{\varphi \mathbf{v}} = 0$.

8.3. Radial and Edge Shape Operators for the Image

Although (M', V) need not be a medial axis, the radial and edge shape operators are still defined. We can compute them using the original operators for (M, U) and the distortion operators (see Damon (2004), Theorem 4.5).

Theorem 8.4. *Suppose (M', V) is the image of a 1D or 2D medial axis (M, U) under the local diffeomorphism φ. Then, with the preceding notation*

(1) *For a non-edge point $x_0 \in M$, the radial shape operator $S_{\mathbf{v}'}$ at $x_0' = \varphi(x_0)$ (for the basis $\mathbf{v}'$ from the parametrization $X_1 = \varphi \circ X$) is given by*

$$S_{\mathbf{v}'} = \sigma(S_{\mathbf{v}} + Q_{\varphi \mathbf{v}}) \tag{8.10}$$

(2) *For a 2D medial axis and a point $x_0 \in \partial M$, we may compute the edge shape operator $S_{E\mathbf{v}'}$ at $x_0' = \varphi(x_0)$ by*

$$S_{E\mathbf{v}'} = \sigma(S_{E\mathbf{v}} + Q_{E\varphi,\mathbf{v}} + E_{\varphi \mathbf{v}}) \tag{8.11}$$

We give a corollary ensuring that the image (M', V) satisfies the radial curvature and edge conditions. First, if M is 1-dimensional then $Q_{\varphi \mathbf{v}} = (q)$, and by Example 2.3 the edge condition reduces to $\frac{\partial V_1}{\partial s} \cdot \mathbf{n}' \neq 0$ If M is 2-dimensional, we let b_i, $i = 1, 2$ denote the eigenvalues of $S_{\mathbf{v}} + Q_{\varphi \mathbf{v}}$ and d the generalized eigenvalue of $((S_{E\mathbf{v}} + Q_{E\varphi,\mathbf{v}} + E_{\varphi,\mathbf{v}}), I_{1,1})$. As in Example 2.4 we compute

$$d = (c_1 + c_{\mathbf{n}1} c_{\mathbf{n}})^{-1} \det(S_{E\mathbf{v}} + Q_{E\varphi,\mathbf{v}} + E_{\varphi,\mathbf{v}})$$

Then, we have as a corollary

Corollary 8.5. *Consider the situation of Theorem 8.4. If M is a 1D medial axis, then (M', V) satisfies the Radial Curvature Condition iff at all non-edge points of M*

$$r < \frac{1}{\kappa_r + q} \quad \text{if } \kappa_r + q > 0 \text{ and no condition otherwise} \tag{8.12}$$

If M is 2-dimensional, then (M', V) satisfies the Radial Curvature Condition iff at all non-edge points of M

$$r < \min\left\{\frac{1}{b_i}\right\} \quad \text{for all positive eigenvalues } b_i \text{ of } S_{\mathbf{v}} + Q_{\varphi v} \tag{8.13}$$

Also, (M', V) satisfies the Edge Condition iff at all points of ∂M,

$$r < \frac{1}{d} \quad \text{if } d > 0 \text{ and no condition otherwise} \tag{8.14}$$

where d is the generalized eigenvalue of $((S_{E\mathbf{v}} + Q_{E\varphi,\mathbf{v}} + E_{\varphi,\mathbf{v}}), I_{1,1})$

Then, provided the image (M', V) satisfies the local initial conditions of Damon (2003), Definition 1.7, then (M', V) is a skeletal structure. We can first apply Corollary 8.5 and radial rigidity at the singular points to be able to apply Theorem 2.5 to conclude that the boundary $\mathcal{B}'$ is smooth. If moreover φ is radially rigid on M, then $\mathcal{B}'$ is (partially) Blum so we can apply Theorem 8.4 together with Theorems 3.1, 3.4, and 4.2 to determine the geometry of $\mathcal{B}'$.

9. Summary

To use the Blum medial axis as a tool for analyzing the shapes and properties of objects, it is desirable to be able to perform operations on medial axes and deduce properties of the resulting associated boundaries. In this paper we have introduced medial structures, namely the radial and edge shape operators and the compatibility 1-form, which allow us to determine that the associated boundary is smooth and then deduce its geometric properties. These operators provide formulas for the geometry of the boundary without explicitly using the differential geometry of the medial axis. Several advantages of this approach are:

(1) The methods are dimension independent.
(2) The expressions for the differential geometric invariants are directly defined on the medial axis.
(3) The invariants naturally decouple the radial distance r from the purely directional information contained in the unit radial vector field U_1.
(4) The expressions we obtain are simpler then those obtained from other approaches, and we specifically justify this claim.
(5) Both intrinsic and relative geometric invariants can be determined.

We further demonstrate the advantage of this approach by constructing on the medial axis a geometric medial map using only the unit radial vector field. This map has an intrinsic component which directly identifies the intrinsic geometry of the boundary and a relative part which identifies the relative geometry of the boundary. We illustrate the usefulness of the methods by computing how the medial data changes when the medial axis is deformed by a diffeomorphism. We identify distortion operators which determine how much the shape operators are changed under the diffeomorphism.

These results have a number of potential applications including: fitting boundary surfaces by medial models, determining properties of deformed regions in terms of deformation properties of the medial axis, identifying special boundary regions in terms of medial data, etc. Optimality criteria for such problems are often expressed by global integrals. Hence, the radial shape operator again appears via the methods in Damon (for Publication) for computing such integrals as related integrals over the medial axis.

References

Bogaevski, I. 2002. Perestroikas of shocks and singularities of minimum functions. *Physica D*, 173:1–28.

Blum, H. and Nagel, R. 1978. Shape description using weighted symmetric axis features. *Pattern Recognition*, 10:167–180.

Bruce, J.W. Giblin, P.J., and Gibson, C.G. 1983. Symmetry sets. *Proc. Roy. Soc. Edinburgh*, 101A: 163–186.

Bruce, J.W. and Giblin, P.J. 1986. Growth, motion, and 1-parameter families of symmetry sets. *Proc. Roy. Soc. Edinburgh*, 104A:179–204.

Bruce, J.W., Giblin, P.J., and Tari, F. 1986. Ridges, crests, and subparabolic lines of evolving surfaces. *Int. Jour. Comp. Vision*, 18(3):195–210.

Damon, J. 2003. Smoothness and geometry of boundaries associated to skeletal structures I: Sufficient conditions for smoothness. *Annales Inst. Fourier*, 53:1941–1985.

Damon, J. 2004. Smoothness and Geometry of Boundaries Associated to Skeletal Structures II: Geometry in the Blum case. *Compositio Mathematica*, 140(6):1657–1674.

Damon, J. 1998. Generic structure of two dimensional images under Gaussian blurring. *SIAM Jour. Appl. Math*, 59:97–138

Damon, J. 1999. Properties of ridges and cores for two dimensional images. *Jour. Math. Imag. and Vision*, 10:163–174.

Damon, J. *Generic Geometry of Functions*. In preparation.

Damon, J. *Global Geometry of Regions and Boundaries via Skeletal and Medial Integrals*. Submitted for publ.

Eberly, D. 1996. *Ridges in Image and Data Analysis. Series in Computational Imaging and Vision Series*. Kluwer Academic Publishers Doordrecht, the Netherlands.

Giblin, P.J. 2000. Symmetry sets and medial axes in two and three dimensions. The Mathematics of Surfaces, Roberto Cipolla and Ralph Martin (eds.), Springer-Verlag, pp. 306–321.

Gibson, C.G. et al. 1976. Topological stability of smooth mappings. Springer Lecture notes in Math. 552:Springer-Verlag.

Golubitsky, M. and Guillemin, V. 1974. *Stable Mappings and their Singularities. Springer Graduate Texts in Mathematics*. Springer-Verlag, Berlin-Heidelberg.

Keller R. 1999. Generic transitions of relative critical sets in parametrized families with applications to image analysis. Ph.D. Thesis, Dept. Math., Univ. of North Carolina.

Kimia, B.B., Tannenbaum, A., and Zucker, S. 1990. Toward a computational theory of shape: An overview. In *Three Dimensional Computer Vision*, O. Faugeras (ed.), MIT Press.

Mather, J. 1973. Stratifications and mappings. In *Dynamical Systems*, M. Peixoto (ed.), Academic Press: New York.

Mather, J. 1983. Distance from a manifold in Euclidean space, in *Proc. Symp. Pure Math*, vol 40 Pt 2, 199–216.

Miller, J. 1998. Relative critical sets in $\mathbb{R}^n$ and applications to image analysis. Ph.D. Thesis, Dept. Math., Univ. of North Carolina.

Nackman L.R. 1982. Three dimensional shape description using the symmetric axis transform. Ph.D. Thesis, Department of Computer Science, University of North Carolina.

Nackman, L.R. and Pizer, S. 1985. Three dimensional shape description using the symmetric axis transform I; Theory. *IEEE PAMI*, 7(2):187–202.

Pizer, S., Eberly, D. et al. 1998. Zoom-invariant vision of figural shape: The mathematics of cores comp. *Vision and Image Understanding*, 69:55–71.

Pizer, S. et al. 2003. Deformable M-reps for 3D medical image segmentation. *Int. Jour. Comp. Vision*, 55(2/3):85–106.

Pizer, S. et al. 1999. Multiscale medial shape-based analysis of image objects. *IEEE Trans. Med. Imaging*, 18:851–865.

Pizer, S. et al. 2003b. Multiscale medial loci and their properties. *Int. Jour. Comp. Vision*, 55(2/3):155–179.

Siddiqi, K., Bouix, S., Tannenbaum, A., and Zucker, S. 2002. The Hamilton-Jacobi skeleton. *Int. Jour. Comp. Vision*, 48(3):215–231

Siersma, D. 1999. Properties of conflict sets in the plane. Geometry and topology of caustics—caustics 1998. Banach Center Publ., 50:267–276.

Sotomayor, J., Siersma, D., and Garcia R. 1999. Curvatures of conflict surfaces in euclidean 3-space geometry and topology of caustics—caustics 1998. Banach Center Publ., 50:277–285.

Szekely, G., Naf, M., Brechbuhler, Ch., and Kubler, O. 1994. Calculating 3d Voronoi diagrams of large unrestricted point sets for skeleton generation of complex 3d shapes. In *Proc. 2nd*

Int. Workshop on Visual Form, World Scientific Publ., pp. 532–541.

Van Manen, M. 2003a. *Curvature and Torsion Formulas for Conflict Sets. Caustics '02 (Warsaw)*. Polish Acad. Sciences Warsaw.

Van Manen, M. 2003b. The geometry of conflict sets. Ph.D. Thesis, Dept. of Mathematics, Univ. of Utrecht.

Yomdin, J. 1981. On the local structure of the generic central set. *Compositio. Math.*, 43:225–238.

Yushkevich, P., Fletcher, T. et al 2002. Continuous medial representations for geometric object modeling in *2D and 3D*. In *Proc. First Generative Model Based Workshop*, Copenhagen, pp. 11–19 and *Image and Vision Computing*, 21:17–27 (2003).